On the Solutions of the Fractional Generalized Gierer–Meinhardt Model

Alessandra Jannelli and Maria Paola Speciale

Abstract In this chapter, we consider a time-fractional generalized Gierer–Meinhardt model described by a system of two coupled nonlinear time-fractional reaction–diffusion equations. Solutions are computed by applying a procedure that combines the Lie symmetry analysis with classical numerical methods. Lie symmetries reduce the target system into time-fractional coupled ordinary differential equations. The numerical solutions are determined by introducing the Caputo definition fractional derivative and by using an implicit classical numerical method. Numerical results are presented to validate the effectiveness of the proposed approach and to show, by a comparison with the integer-order case, that the fractional-order model can be considered a reliable generalization of the classical model.

1 Introduction

In this chapter, we consider a system of two coupled nonlinear time-fractional reaction–diffusion (TF–RD) equations

$$\begin{cases} \partial_t^\alpha u(t,x) = k_1 \partial_{xx} u(t,x) + f(t,x,u,v), \\ \partial_t^\alpha v(t,x) = k_2 \partial_{xx} v(t,x) + g(t,x,u,v), \end{cases} \quad 0 < \alpha < 1, \tag{1}$$

subject to suitable initial and boundary conditions. In (1), ∂_t^α is the Riemann–Liouville fractional derivative operator [1–4]

$$\partial_t^\alpha w(t,x) = \frac{1}{\Gamma(1-\alpha)} \frac{\partial}{\partial t} \int_0^t \frac{w(s,x)}{(t-s)^\alpha} ds.$$

A. Jannelli (✉) · M. P. Speciale (✉)
Department of Mathematical and Computer Sciences, Physical Sciences and Earth Sciences, University of Messina, Messina, Italy
e-mail: ajannelli@unime.it; mpspeciale@unime.it

© The Author(s), under exclusive license to Springer Nature Singapore Pte Ltd. 2023

A. Cardone et al. (eds.), *Fractional Differential Equations*,
Springer INdAM Series 50, https://doi.org/10.1007/978-981-19-7716-9_6

$u(t,x)$ and $v(t,x)$ are the field variables at time t and position x. $k_1 > 0$ and $k_2 > 0$ the diffusion coefficients of $u(t,x)$ and $v(t,x)$, respectively. The functions $f = f(t,x,u,v)$ and $g = g(t,x,u,v)$ represent the nonlinear interaction terms.

The system (1) has been proved to be a strong tool in the modeling of many physical and chemical phenomena [5–14]. Many mathematical models have been proposed in different fields of the applied sciences, and their analytical and numerical solutions have been extensively investigated. In 1972, Gierer and Meinhardt [15] proposed a prototypical depletion-type chemical model, which is described as follows:

$$\begin{cases} \partial_t u(t,x) = k_1 \partial_{xx} u(t,x) + c_1 u + d_1 \rho_1(x) \dfrac{u^p}{v^q} + \sigma_1, \\ \partial_t v(t,x) = k_2 \partial_{xx} v(t,x) + c_2 v + d_2 \rho_2(x) \dfrac{u^r}{v^s} + \sigma_2, \end{cases} \tag{2}$$

where the involved parameters are assigned constants, except for the distributions ρ_1 and ρ_2, which instead are assigned functions of the space variable x. It describes the interaction between two substances, the activator $u(t,x)$ and the inhibitor $v(t,x)$, and it is commonly used to explain the underlying complex mechanism for pattern formation in nature, describing the interaction of two sources in processes such as biological and chemical ones.

In this chapter, we propose a time-fractional model, generalization of the above classical Gierer–Meinhardt model (2), given by the fractional system (1) assuming the nonlinear interaction terms as follows:

$$\begin{aligned} f(t,x,u,v) &= c_1 u + d_1 \rho_1(x) \frac{u^p}{v^q} + \sigma_1(t,x) \\ g(t,x,u,v) &= c_2 v + d_2 \rho_2(x) \frac{u^r}{v^s} + \sigma_2(t,x) \end{aligned} \tag{3}$$

according to the source terms involved in the Gierer and Meinhardt model (2), but with $\sigma_1(t,x)$ and $\sigma_2(t,x)$ arbitrary functions of time and space. We study the mathematical model in which the fractional order involves the time derivative. Unlike other works (see, for instance, [16–20]) in which models describing space-fractional reaction–diffusion equations with anomalous diffusion process are investigated, in this work, we focus on a mathematical model in which the fractional order involves the time derivative. In particular, we analyze the model when $p = r = 2$ and $s = q = -1$, that when $\alpha = 1$ describes a depletion process where the autocatalysis is counteracted by the depletion of a substrate of the concentration $v(x,t)$ required for activation $u(t,x)$. This model was used to describe pigmentation patterns in seashells and the ontogeny of ribbing on ammonoid shells [21, 22]. The stability, the Hopf bifurcation and the Turing instability by the technique of stability theory, normal form theory, and center manifold reduction were carried out in [23, 24].

The main aim of this study is to solve the proposed fractional generalized mathematical model by applying a procedure that combines the Lie symmetry analysis with the numerical methods. It was applied to a wide class of FDES: space-fractional

advection–diffusion–reaction equations with linear [25] and nonlinear sources terms [26], a system of time-fractional advection–diffusion–reaction equations (1) with arbitrary nonlinear source terms [27] and two-dimensional time-fractional reaction–diffusion equations [28, 29].

The authors choose to approach the study of the target model initially by considering the Riemann–Liouville derivative since it is widely used in the context of the group method. The fractional Lie symmetries are determined by using a package of symbolic computing: FracSym on MAPLE platform, an algorithmic that automates the method, which is an extension of classical Lie symmetries approach to FPDEs [30, 31], of finding symmetries for FPDEs with Riemann–Liouville fractional derivative [32, 33]. By using the Lie symmetries, the target system is mapped into a system of time-fractional ordinary differential equations, and by solving the reduced FODEs, exact and numerical solutions are found. The numerical solutions are computed by introducing the Caputo definition fractional derivative and by using an implicit classical numerical method. The Caputo definition of the fractional derivative allows defining an initial value problem whose the initial conditions are given in terms of the field variable and of its integer-order derivatives, in agreement with the clear physical meaning of most of the processes arising in the real world.

We want to remark that, in this context, we are not interested in studying the stability of the model, or in the effects of diffusion on the stability of equilibrium points, or to explore the dynamical behaviors induced by diffusion or the bifurcated limit cycle from the bifurcation, topics widely studied in the specialized literature. Our aim is to find analytical and numerical solutions of the generalized mathematical model with fractional derivatives (1)–(3), in order to show the effectiveness of the proposed model and of the procedure that reveals to be a good tool for solving a wide class of fractional partial differential equations (FPDEs).

In Sect. 2, we introduce the Lie transformation that reduces the target system into time-fractional ordinary differential equations. In Sect. 3, we search for analytical solutions for the fractional generalized depletion model. In Sect. 4, by introducing the Caputo definition of the fractional derivative and by using an implicit classical trapezoidal method, the numerical solutions are found. In Sect. 5, we report concluding remarks.

2 Lie Transformation and FODEs

Analytical and numerical solutions of the mathematical model are found by applying a procedure that combines the Lie symmetry analysis with the numerical methods: by using the extension of Lie symmetries approach to FPDEs [30, 31], we find the Lie fractional symmetries admitted by the model and, then, Lie transformations that map the system of coupled nonlinear TF-RD equations (1) into a system of fractional ordinary differential equations (FODEs). By solving the reduced FODEs, we obtain solutions of the original model.

In this section, we present the Lie transformation that maps (1), with the reactions (3), into a system of two coupled FODEs. The Lie transformations of the system (1) with arbitrary sources terms were recently determined in [27] and assume the following form, according to the choice of source terms given by (3)

$$T = t, \qquad U = u(t,x)e^{-a_1 x}, \qquad V = v(t,x)e^{-a_2 x}\,, \tag{4}$$

where a_1 and a_2 are arbitrary constants and

$$\begin{aligned} \rho_1(x) &= e^{(a_1(1-p)+a_2 q)x}\rho_1' \qquad & \sigma_1(T,x) &= e^{a_1 x}h_1(T) \\ \rho_2(x) &= e^{(a_2(s+1)-a_1 r)x}\rho_2' & \sigma_2(T,x) &= e^{a_2 x}h_2(T), \end{aligned} \tag{5}$$

with ρ_1' and ρ_2' arbitrary constants and $h_1 = h_1(T)$ and $h_2 = h_2(T)$ arbitrary functions of their argument. The above transformations lead the source terms to assume the following form:

$$\begin{aligned} f(t,x,u,v) &= c_1 u + d_1 e^{(a_1(1-p)+a_2 q)x}\frac{u^p}{v^q} + h_1(t)e^{a_1 x}, \\ g(t,x,u,v) &= c_2 v + d_2 e^{(-a_1 p+a_2(q+1))x}\frac{u^p}{v^q} + h_2(t)e^{a_2 x}. \end{aligned} \tag{6}$$

Note that the functional forms of the distributions, ρ_1 and ρ_2, consistent with ones of the classical model of Gierer–Meinhardt [15], and the additional terms, σ_1 and σ_2 depending also on variables t and x, lead us to define the target model as a generalization of the model studied in [15].

When the transformation (4) and the above forms of ρ_1, ρ_2, σ_1, and σ_2 are inserted into the system (1) with sources terms given by (3), it is reduced into the following system of fractional nonlinear ordinary differential equations:

$$D_T^\alpha U - (c_1 + k_1 a_1^2)U - \frac{U^p}{V^q}d_1 - h_1 = 0 \tag{7}$$

$$D_T^\alpha V - (c_2 + k_2 a_2^2)V - \frac{U^r}{V^s}d_2 - h_2 = 0 \tag{8}$$

setting $\rho_1' = \rho_2' = 1$. The choice of the arbitrary functions h_1 and h_2 characterizes the solutions of the equations (7) and (8) and, then, the class of solutions given by (4).

In order to solve the system (7) and (8), we assume $p = r$ and $s = q$. Multiplying (7) by d_2 and (8) by $-d_1$ and, then, adding the equations, we get the following fractional ordinary differential equation (FODE):

$$D_T^\alpha(d_2 U - d_1 V) - (c_1 + k_1 a_1^2)(d_2 U - d_1 V) - (d_2 h_1 - d_1 h_2) = 0, \tag{9}$$

where we set $c_2 + k_2 a_2^2 = c_1 + k_1 a_1^2$. Under non-vanishing initial condition

$$\lim_{T \to 0} D_T^{\alpha-1}(d_2 U(T) - d_1 V(T)) = b^0, \tag{10}$$

the FODE (9) admits the following analytical solution:

$$\begin{aligned} U(T) = &\frac{d_1}{d_2} V + \frac{b^0}{d_2} T^{\alpha-1} E_{\alpha,\alpha}(\lambda T^\alpha) \\ &+ \int_0^T (T-S)^{\alpha-1} E_{\alpha,\alpha}(\lambda (T-S)^\alpha)(h_1 - \frac{d_1}{d_2} h_2) dS, \end{aligned} \tag{11}$$

where $\lambda = c_1 + k_1 a_1^2$. Substituting $U(T)$ in (8), we get the following FODE:

$$\begin{aligned} &D_T^\alpha V - \lambda V - d_2^{1-p} \\ &\frac{\left(d_1 V + b^0 T^{\alpha-1} E_{\alpha,\alpha}(\lambda T^\alpha) + \int_0^T (T-S)^{\alpha-1} E_{\alpha,\alpha}(\lambda (T-S)^\alpha))(h_1 d_2 - h_2 d_1) dS\right)^p}{V^q} \\ &- h_2 = 0, \end{aligned} \tag{12}$$

subject to the non-vanishing initial condition

$$\lim_{T \to 0} D_T^{\alpha-1} V(T) = V^0. \tag{13}$$

By solving the initial values problem (12)–(13), we find the solution $V(T)$ and, as consequence, by (11) the solution $U(T)$ and, finally, by the inverse transformations (4) the solutions $u(t, x)$ and $v(t, x)$ of the proposed system of FPDEs (1) with source terms given by (6) and with the initial conditions

$$\lim_{t \to 0} \partial_t^{\alpha-1} u(t, x) = \frac{b^0 - d_1 V^0}{d_2} e^{a_1 x}, \qquad \lim_{t \to 0} \partial_t^{\alpha-1} v(t, x) = V^0 e^{a_2 x}. \tag{14}$$

The target model describes a generalized depletion process when $p = 2$ and $q = -1$, and this will be the object of the analysis in the next section.

3 Analytical Solutions of the Generalized Depletion Model

In order to find solutions of the generalized depletion model, we choose the functions $h_1(T)$ and $h_2(T)$ in (12) by setting the parameters $b_0 = 0$ and $\lambda = 0$

so that Eq. (12) reads

$$D_T^{\alpha} V - \frac{1}{d_2}\left(d_1 V + \frac{1}{\Gamma(\alpha)}\int_0^T (T-S)^{\alpha-1}(h_1 d_2 - h_2 d_1) dS\right)^2 V - h_2 = 0. \quad (15)$$

We set

$$h_1(T) = \frac{d_1}{d_2} h_2(T) - \frac{h_0(T)}{d_2},$$

with $h_0(T)$ arbitrary function of T, and we obtain

$$D_T^{\alpha} V - \frac{1}{d_2}\left(d_1 V - \frac{1}{\Gamma(\alpha)}\int_0^T (T-S)^{\alpha-1} h_0(S) dS\right)^2 V - h_2 = 0. \quad (16)$$

The involved arbitrary function $h_2(T)$ is assigned in such a way that the FODE (16) admits analytical solutions for $\alpha = 1$.

1. We set

$$h_2(T) = Be^{-AT} \left((1-AT) - \frac{t}{d_2}\left(d_1 BTe^{-AT} - \frac{1}{\Gamma(\alpha)}\int_0^T (T-S)^{\alpha-1} h_0(S) dS\right)^2\right) \quad (17)$$

with A and B arbitrary constants. With the above choice of the function $h_2(T)$ and when $\alpha = 1$, we get the following exact solution;

$$V(T) = BTe^{-AT},$$

and substituting it in (11) we obtain

$$U(T) = \frac{1}{d_2}\left(d_1 BTe^{-AT} - \int_0^T h_0(S) dS\right).$$

By means of the inverse transformations (4), we get the exact solution of the generalized depletion Gierer–Meinhardt model

$$u(t,x) = e^{a_1 x}\frac{1}{d_2}\left(d_1 Bte^{-At} - \int_0^t h_0(s) ds\right),$$
$$v(t,x) = e^{a_2 x} Bte^{-At}.$$

2. We set

$$h_2(T) = \frac{A}{\cosh^2(T)} + \frac{1}{d_2}(B + A\tanh(T))$$
$$\left(d_1(B + A\tanh(T)) - \frac{1}{\Gamma(\alpha)}\int_0^T (T-S)^{\alpha-1} h_0(S)dS\right)^2. \quad (18)$$

By the above choice of function h_2 and when $\alpha = 1$, we get the following exact solution:

$$V(T) = B + A\tanh(T),$$

and substituting it in (11), we obtain

$$U(T) = \frac{1}{d_2}\left(d_1(B + A\tanh(T)) - \int_0^T h_0(S)dS\right).$$

By means of the inverse transformations (4), we get the exact solution of the generalized depletion Gierer–Meinhardt model

$$u(t,x) = e^{a_1 x}\frac{1}{d_2}\left(d_1(B + A\tanh(t)) - \int_0^t h_0(s)ds\right),$$
$$v(t,x) = e^{a_2 x}(B + A\tanh(t)).$$

In the next section, starting from the expressions of $h_1(T)$ and $h_2(T)$ reported in the above examples, and setting $h_0(T)$, we get numerical solutions of the fractional generalized depletion model.

4 Numerical Method and Solutions

In this section, we find the numerical solutions of the system of FPDEs (1) computed by solving the FODE (16), obtained in the above section by a suitable choice of the involved parameters and functions and where the function $h_2(T)$ is given by (17) or (18). Computed the numerical solution $V(T)$, we obtain the numerical solution $U(T)$ by (11) and then the solutions $u(t,x)$ and $v(t,x)$ of the target model (1) by the inverse transformations by (4).

We introduce the α-order Caputo fractional derivative of the solution $V(T)$

$${}^C D_T^\alpha V(T) = \frac{1}{\Gamma(1-\alpha)}\int_0^T (T-S)^{-\alpha} V'(S)dS$$

and its connection with the α-order Riemann–Liouville fractional derivative [1]

$$ {}^{C}D_T^{\alpha} V(T) = D_T^{\alpha} \left(V(T) - V(0) \right), $$

with $V(0)$ initial condition. In terms of the Caputo derivative, the following fractional initial value problem (FIVP) is obtained:

$$ \begin{aligned} &{}^{C}D_T^{\alpha} V(T) = F(T, V), \quad 0 < \alpha < 1 \\ &V(0) = V^0, \end{aligned} \tag{19} $$

where

$$ F(T, V) = -\frac{V^0}{\Gamma(1-\alpha) T^{\alpha}} + \frac{1}{d_2} \left(d_1 V - \frac{1}{\Gamma(\alpha)} \int_0^T (T - S)^{\alpha - 1} h_0(S) dS \right)^2 V + h_2 $$

and

$$ h_0(T) = \frac{h}{(1 + T^2)^{1.5}} \tag{20} $$

with h arbitrary constant. We remark that the Caputo definition of the fractional derivative allows defining an FIVP whose the initial conditions are given in terms of the field variable and of its integer-order derivatives, in agreement with the clear physical meaning of most of the processes arising in the real world.

In order to numerically solve the FIVP (19), we propose the classical implicit trapezoidal method (PI_2 Im), an efficient numerical method used for its good stability and accuracy properties [4, 34], numerical results by multi-steps methods are presented in [18]. We build a computational uniform mesh of $N + 1$ grid points denoted by T^n, with $T^n = T^0 + n\Delta T$ and integration step sizes ΔT and N positive integer. We denote by U^n the numerical approximation provided by the numerical method of the exact solution $U(T^n)$ at the mesh points T^n, for $n = 0, \cdots, N$. The numerical method reads

$$ V^{n+1} = V^0 + \frac{1}{\Gamma(\alpha)} \left(\beta_0 F(T^0, V^0) + \sum_{k=1}^{n+1} \beta_k F(T^k, V^k) \right), \tag{21} $$

where the coefficient values β_k, for $k = 0, \cdots, n + 1$, are computed as follows:

$$ \beta_0 = \frac{1}{\alpha(\alpha + 1)} \frac{(T^{n+1})^{\alpha} ((T^1 - T^0)(\alpha + 1) - T^{n+1}) + (T^{n+1} - T^1)^{\alpha + 1}}{T^1 - T^0}, $$

$$ \beta_k = \frac{1}{\alpha(\alpha + 1)} \times \qquad k = 1, \cdots, n, $$

$$\times \left(\frac{(T^{n+1} - T^{k-1})^{\alpha+1} - (T^{n+1} - T^{k})^{\alpha+1}}{T^{k} - T^{k-1}} \right.$$
$$\left. - \frac{(T^{n+1} - T^{k})^{\alpha+1} - (T^{n+1} - T^{k+1})^{\alpha+1}}{T^{k+1} - T^{k}} \right),$$

$$\beta_{n+1} = \frac{1}{\alpha(\alpha+1)} (T^{n+1} - T^{n})^{\alpha} .$$

The convergence order of the scheme is $O((\Delta T)^{min(1+\alpha,2)})$. Note that the convergence order of the trapezoidal method usually is $1+\alpha$ when $0 < \alpha < 1$. Only when $\alpha > 1$ or when the solution is sufficiently smooth, we obtain the reached order 2 [34]. In general, the numerical method (21) leads to obtain a nonlinear equation at each step for whose resolution a root-finding solver is needed. The classical Newton method is proposed.

In the following, we report two test problems characterized by the function $h_2(T)$, given by (17) or (18). Different simulation parameters, involved functions, and α parameter values are considered as the input features of the model under study. The exact solutions for $\alpha = 1$, reported in Sect. 3, are considered as reference ones for testing qualitative behavior of the numerical solutions of the models for values of the α parameter increasing toward 1. All numerical simulations are performed on Intel Core i7 by using Matlab 2020 software.

Example 1 In this example, we consider the FIVP (19) with $V^0 = 0$ and

$$h_2(T) = Be^{-AT} \left((1 - AT) - \frac{T}{d_2} \left(d_1 BTe^{-AT} - \frac{1}{\Gamma(\alpha)} \int_0^T \frac{h(T-S)^{\alpha-1}}{(1+S^2)^{1.5}} dS \right)^2 \right).$$

For $\alpha = 1$, the analytical solution $V(T)$ is given by

$$V(T) = BTe^{-AT}, \tag{22}$$

and then, we are able to compute the analytical solution $U(T)$

$$U(T) = \frac{1}{d_2} \left(d_1 BTe^{-AT} - \frac{hT}{\sqrt{1+T^2}} \right). \tag{23}$$

We choose a computational domain $[0, T_{max}]$ with $T_{max} = 10$ and $N = 100$ grid points and set the parameters values as follows: $d_1 = 0.00016$, $d_2 = -0.00048$, $A = 2$, $B = 0.02$, and $h = 0.0001$. We remark that, in this example, the parameters values are chosen according to the values by Gierer and Meinhardt reported in [15], values ensuring that the model is a well-posed one, with the aim to validate our numerical results obtained by the proposed procedure.

In Fig. 1, we report the numerical results obtained for different values of the α parameter: in the left frame, the numerical solution V^n obtained by solving the FIVP

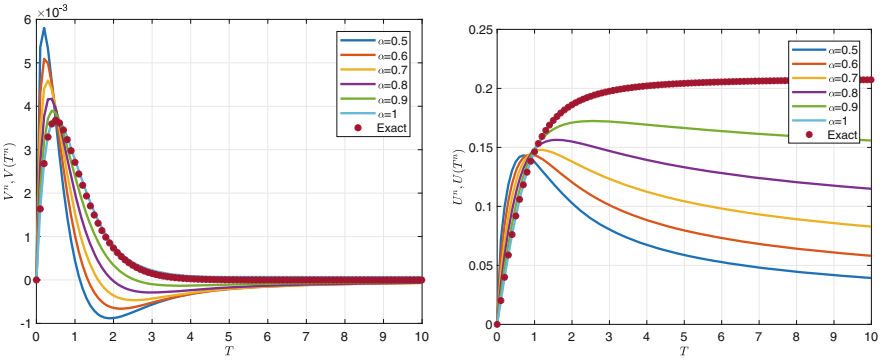

Fig. 1 Numerical solutions for different values of α. Left frame: numerical solution V^n of the FIVP (19). Right frame: numerical solution U^n computed by (11)

(19) by using the PI_2 Im numerical method, and in the right frame, the numerical solution U^n computed by means of (11) by the suitable substitution of the involved functions and parameters

$$U^n = \frac{1}{d_2}\left(d_1 V^n - T\ {}_3F_2([0.5, 1, 1.5]; [(1+\alpha)/2, 1+\alpha/2]\,; -(T^n)^2)\right)$$

and given in terms of the generalized hypergeometric function ${}_pF_q(a; b; z)$ of order p, q defined as follows:

$$\begin{aligned} {}_pF_q(a; b; z) &= {}_pF_q([a_1, a_2, \ldots, a_p]; [b_1, b_2, \ldots, b_q]; z) \\ &= \sum_{n=0}^{\infty} \left(\frac{(a_1)_n, (a_2)_n, \ldots, (a_p)_n}{(b_1)_n, (b_2)_n, \ldots, (b_q)_n}\right)\left(\frac{z^2}{n!}\right) \end{aligned}$$

with $a = [a_1, a_2, \ldots, a_p]$ and $b = [b_1, b_2, \ldots, b_q]$ vectors of lengths p and q, respectively. $(a)_k$ and $(b)_k$ represent the Pochhammer symbols defined in the following way:

$$(w)_m = \frac{\Gamma(w+m)}{\Gamma(w)}.$$

The red dot points represent the exact solutions $V(T)$, given by (22), and $U(T)$, given by (23), of the model with $\alpha = 1$. They are reported in order to test the qualitative behavior of the numerical solutions as the α parameter increases toward 1. The solutions reveal very different behavior: both start from the value 0, and both increase at the beginning of the integration process. After, as time evolves, the solution $U(T)$ increases and converges to a constant state. The solution $V(T)$ decreases and converges to zero. Note that, as the value of α increases, for $T < 1$ both solutions decrease and, then, for $T > 1$ increase. The qualitative behavior of

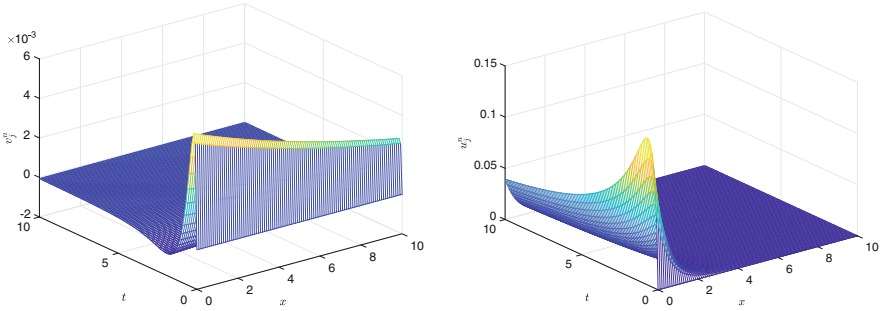

Fig. 2 Numerical solutions of the system of FPDE (1) for $\alpha = 0.5$. Left frame: numerical solution v_j^n. Right frame: numerical solution u_j^n

the solutions is in agreement with one of the classical depletion models. This means that the proposed mathematical model can represent a good generalization of the classical model.

In Fig. 2, we report the numerical solutions u_j^n and v_j^n, approximations of the exact solutions obtained by the inverse transformations (4)

$$u(t,x) = U(t)e^{a_1 x}, \qquad v(t,x) = V(t)e^{a_2 x},$$

solutions of the model (1) integrated with the initial and boundary conditions obtained by (14) with $V^0 = 0$ and $b^0 = 0$ and computed for $\alpha = 0.5$. In this contest, the source terms assume the following form:

$$f(t,x,u,v) = c_1 u + d_1 e^{-(a_1+a_2)x} uv^2 + h_1 e^{a_1 x},$$
$$g(t,x,u,v) = c_2 v + d_2 e^{-2a_1 x} uv^2 + h_2 e^{a_2 x}.$$

The parameters are chosen in the following way: $a_1 = -\sqrt{-c_1/k_1}$, $a_2 = -\sqrt{-c_2/k_2}$ with $k_1 = 10^{-3}$, $k_2 = 0.45$, and $c_1 = c_2 = -0.0025$. The computational domain is given by $[0, T_{max}] \times [0, X_{max}]$ with $T_{max} = 10$, $X_{max} = 10$, and $N = J = 100$ grid points.

Example 2 In this example, we consider the FIVP (19) with $V^0 = 0$ and

$$h_2(T) = \frac{A}{\cosh^2(T)} + \frac{1}{d_2}(B + A\tanh(T)) \left(d_1(B + A\tanh(T)) - \frac{1}{\Gamma(\alpha)} \int_0^T \frac{h(T-S)^{\alpha-1}}{(1+S^2)^{1.5}} dS \right)^2.$$

For $\alpha = 1$, the analytical solution of the FIVP is given by

$$V(T) = B + A\tanh(T), \tag{24}$$

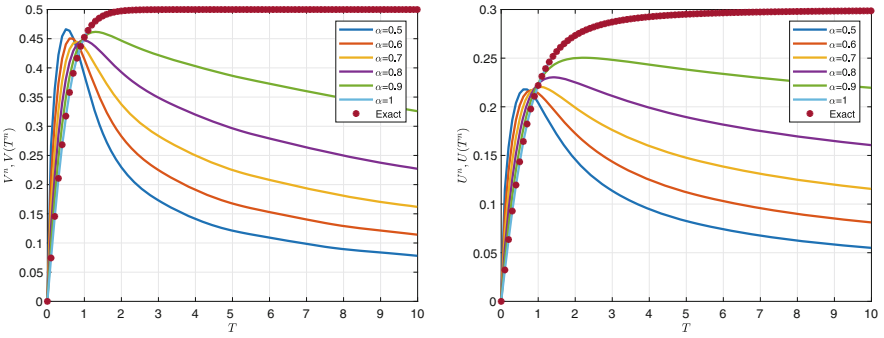

Fig. 3 Numerical solutions for different values of α. Left frame: Numerical solution V^n of the FIVP (19). Right frame: Numerical solution U^n computed by (11)

and then, we are able to compute the analytical solution $U(T)$

$$U(T) = \frac{1}{d_2}\left(B + A\tanh(T) - \frac{hT}{\sqrt{1+T^2}}\right). \tag{25}$$

We set the parameters values as follows: $d_1 = 0.1$, $d_2 = 1$, $A = -0.5$, $B = 0$, and $h = 0.25$. We choose a computational domain $[0, T_{max}]$ with $T_{max} = 10$ and $N = 100$ grid points. In Fig. 3, we report the numerical results obtained for different values of the α parameter: in the left frame, the numerical solution V^n obtained by solving the FIVP (19) by using the PI_2 Im numerical method; in the right frame, the numerical solution U^n computed by means of (11) in terms of the generalized hypergeometric function. The red dot points represent the exact solution $V(T)$, given by (24), and the exact solution $U(T)$, given by (25), of the model with $\alpha = 1$. In this case, the solutions reveal very similar behavior: both start from the value 0, and both increase at the beginning of the integration process. After, as time evolves, both decrease and converge to a constant state. Note that, as the value of α increases, for $T < 1$ both solutions decrease and, then, for $T > 1$ increase. The qualitative behavior of the solutions is in agreement with the choice of the distributions which are both positive functions of x; in fact, the parameters d_1 and d_2 agree in the sign.

In Fig. 4, we report the numerical solutions u_j^n and v_j^n, approximations of the exact solutions obtained by the inverse transformations (4). The source terms are assigned as before. The parameters are chosen in the following way: $a_1 = -\sqrt{-c_1/k_1}$, $a_2 = -\sqrt{-c_2/k_2}$ with $k_1 = 1$, $k_2 = 10$, and $c_1 = c_2 = -0.2$. The computational domain is given by $[0, T_{max}] \times [0, X_{max}]$ with $T_{max} = 10$, $X_{max} = 10$ and $N = J = 100$ grid points.

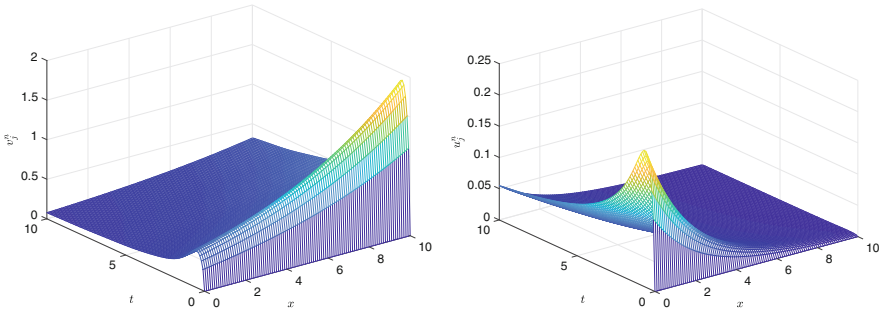

Fig. 4 Numerical solutions of the system of FPDE (1) for $\alpha = 0.5$. Left frame: numerical solution v_j^n. Right frame: numerical solution u_j^n

5 Concluding Remarks

In this study, analytical and numerical solutions for the generalized Gierer–Meinhardt fractional model are presented. We propose a mathematical model governed by a system of two time-fractional diffusion–reaction equations describing the interaction between two chemical substances, commonly used to explain the underlying complex mechanism for pattern formation in nature. The numerical results, obtained by applying the procedure that combines the Lie symmetry analysis with the trapezoidal numerical method, reveal the effectiveness of the proposed model. Moreover, it is important to note that some analytical solutions of the generalized Gierer–Meinhardt model of integer order are found for a suitable choice of the involved parameters and functions. The topic of the next study is the spatial-fractional reaction–diffusion equations with an anomalous diffusion process that occurs in spatially inhomogeneous media.

Acknowledgments A. J. is a member of GNCS-INdAM Research Group. M.P. S. is a member of GNFM-INdAM Research Group.

References

1. Podlubny, I.: Fractional Differential Equations: An Introduction to Fractional Derivatives, Fractional Differential Equations, Some Methods of Their Solution and Some of Their Applications. Academic Press, San Diego (1999)
2. Kilbas, A.A., Srivastava, H.M., Trujillo, J.J.: Theory and Applications of Fractional Differential Equations. North-Holland Mathematics Studies. Elsevier (2006)
3. Samko, S., Kilbas, A.A., Marichev, O.: Fractional Integrals and Derivatives. Taylor and Francis (1993)
4. Diethelm, K.: The Analysis of Fractional Differential Equations. Springer, Berlin (2004)
5. Henry, B.I., Wearne, S.L.: Fractional reaction-diffusion. Physica A, **276**, 448–455 (2000)

6. Seki, K., Wojcik, M., Tachiya, M.: Fractional reaction-diffusion equation. J. Chem. Phys. **119**, 2165 (2003)
7. Gafiychuk, V., Datsko, B.: Pattern formation in a fractional reaction-diffusion system. Phys. A Stat. Mech. Appl. **365**, 300–306 (2006)
8. Gafiychuk, V.V., Datsko, B.Y.: Spatio-temporal pattern formation in fractional reaction-diffusion systems with indices of different order. Phys. Rev. E **77**(6), 066210 (2008)
9. Gafiychuk, V., Datsko, B.: Different types of instabilities and complex dynamics in reaction-diffusion systems with fractional derivatives. J. Comput. Nonlin. Dyn. **7**, 031001 (2012)
10. Datsko, B., Gafiychuk, V.: Complex nonlinear dynamics in subdiffusive activator-inhibitor systems. Commun. Nonlinear Sci. Numer. Simul. **17**, 1673–1680 (2012)
11. Nec, Y.: Explicitly solvable eigenvalue problem and bifurcation delay in sub-diffusive Gierer-Meinhardt model. Eur. J. Appl. Math. **27**(5), 699–725 (2016)
12. Nec, Y.: Spike solutions in Gierer#x2013; Meinhardt model with a time dependent anomaly exponent. Commun. Nonlinear Sci. Numer. Simul. **54**, 267–285 (2018)
13. Jannelli, A.: Numerical solutions of fractional differential equations arising in engineering sciences. Mathematics **8**, 215 (2020)
14. Jannelli, A.: Adaptive numerical solutions of time-fractional advection-diffusion-reaction equations. Commun. Nonlinear. Sci. Numer. Simul. **105**, 106073 (2022)
15. Gierer, A., Meinhardt, H.: A theory of biological pattern formation. Kybernetik **12**, 30–39 (1972); Biological Cybernetics **12**(1), 30–39 (1972). https://doi.org/10.1007/BF00289234
16. Henry, B.I., Wearne, S.L.: Existence of turing instabilities in a two-species fractional reaction-diffusion system. SIAM J. Appl. Math. **62**(3), 870–887 (2002)
17. Henry, B.I., Langlands, T.A.M., Wearne, S.L.: Turing pattern formation in fractional activator-inhibitor systems. Phys. Rev. E Stat. Nonlinear Soft Matter Phys. **72**(2), 026101 (2005)
18. Guo, L., Zeng, F., Turner, I., Burrage, K., Karniadakis, G.E.M.: Efficient multistep methods for tempered fractional calculus: Algorithms and simulations. SIAM J. Sci. Comput. **41**(4), 2510–2535 (2019)
19. Yu, W., Rongpei, Z., Zhen, Zijian, H.: Turing pattern in the fractional Gierer-Meinhardt model. Chin. Phys. B **28**(5), 050503 (2019)
20. Wei, J., Yang, W.: Multi-bump Ground states of the fractional Gierer-Meinhardt system on the real line. J. Dyn. Differ. Equ. **31**, 385–417 (2019)
21. Meinhardt, H., Klingler, M.: A model for pattern formation on the shells of molluscs. J. Theor. Biol. **126**, 63–89 (1987)
22. Buceta, J., Lindenberg, K.: Switching-induced Turing instability. Phys. Rev. E **66**, 046202 (2002)
23. Wu, R., Shao, Y., Zhou, Y., Chen, L.: Turing and Hopf bifurcation of Gierer-Meinhardt activator-substrate model. Electron. J. Differ. Equ. **2017**(173), 1–19 (2017)
24. Chen, L., Wu, R., Xu, Y.: Dynamics of a depletion-type Gierer-Meinhardt model with Langmuir-Hinshelwood reaction scheme. Discrete Contin. Dyn. Syst. B (2020). https://doi.org/10.3934/dcdsb.2021132
25. Jannelli, A., Ruggieri, M., Speciale, M.P.: Numerical solutions of space fractional advection-diffusion equation with source term. AIP Confer. Proc. **2116**, 280007 (2019)
26. Jannelli, A., Ruggieri, M., Speciale, M.P.: Numerical solutions of space fractional advection–diffusion equation, with nonlinear source term. Appl. Num. Math. **155**, 93–102 (2020)
27. Jannelli, A., Speciale, M.P.: On the numerical solutions of coupled nonlinear time-fractional reaction–diffusion equations. AIMS Math. **6**(8), 9109–9125 (2021)
28. Jannelli, A., Speciale, M.P.: Exact and numerical solutions of two-dimensional time–fractional diffusion-reaction equation through the lie symmetries. Nonlinear Dynamics **105**, 2375–2385 (2021)
29. Jannelli, A., Speciale, M.P.: Comparison between Solutions of two-dimensional time-fractional diffusion-reaction equation through the lie symmetries. Atti della Accademia Peloritana dei Pericolanti **99**, A4 (2021)
30. Gazizov, R.K., Kasatkin, A.A., Lukashchuk, S.Y.: Continuous transformation groups of fractional differential equations, Vestn. USATU **9**, 125–35 (2007)

31. Gazizov, R.K., Kasatkin, A.A., Lukashchuk, S.Y.: Group-invariant solutions of fractional differential equations. Nonlinear Sci. Complex. 51–59 (2011)
32. Vu, K.T., Jefferson, G.F., Carminati, J.: Finding generalized symmetries of differential equations using the MAPLE package DESOLVII. Comput. Phys. Commun. **183**, 1044–1054 (2012)
33. Jefferson, G.F., Carminati, J.: ASP: Automated symbolic computation of approximate symmetries of differential equations. Comput. Phys. Commun. **184**, 1045–1063 (2013)
34. Garrappa, R.: Trapezoidal methods for fractional differential equations: Theoretical and computational aspects. Math. Comput. Simul. **110**, 96–112 (2015)